

Projections for Two Higgs Doublet Models at the LHC and ILC: A Snowmass White Paper

Chien-Yi Chen

Department of Physics, Brookhaven National Laboratory, Upton, New York, 11973

(Dated: August 16, 2013)

The discovery of the 125 GeV Higgs boson and the measurement of its branching ratios has initiated the exploration of the electroweak symmetry breaking sector. There have been numerous studies exploring the restrictions these results place on the parameter space of two Higgs doublet models. We extend these results to include the full data set and study the expected sensitivity that can be obtained with 300 fb^{-1} and 3000 fb^{-1} integrated luminosity. In addition, searches for a heavy Standard Model Higgs boson are also considered. It is shown that the nonobservation of such a Higgs boson can substantially narrow the allowed regions of parameter space in two Higgs doublet models. Finally, projections for the ILC at the center of mass energy 250, 500, and 1000 GeV are investigated.

I. INTRODUCTION

The discovery of a Higgs boson at the LHC with a mass around 125 GeV is the beginning of the exploration of the source of electroweak symmetry breaking. Many beyond the Standard Model (SM) scenarios have a Higgs-like particle which has SM-like couplings to fermions and gauge bosons. A well-motivated extension of the SM is obtained by adding a second $SU(2)_L$ Higgs doublet, leading to five physical Higgs scalars: two charged Higgs bosons H^\pm , a pseudoscalar A , and two neutral scalars, h^0 and H^0 . Although it is possible that the 125 GeV state is the heavier neutral Higgs particle, h^0 , of a 2 Higgs doublet model (2HDM) [1–3], we assume here that it is the lighter. Two Higgs doublet models generically have tree level flavor changing neutral currents from Higgs exchanges unless there is a global or discrete symmetry which forbids such interactions[4, 5] and therefore we consider only the class of models where there is a discrete Z_2 symmetry such that one type of the fermions couples only to a single Higgs doublet. There are four possibilities for 2HDMs of this type which are typically called the type-I, type-II, lepton specific, and flipped models[4]. The couplings of the Higgs bosons to fermions are described by two free parameters. The ratio of vacuum expectation values of the two Higgs doublets is $\tan\beta \equiv \frac{v_2}{v_1}$, and the mixing angle which diagonalizes the neutral scalar mass matrix is α . The couplings of a neutral CP-even Higgs (ϕ^0) to the SM particles are parametrized as

$$\mathcal{L} = - \sum_f g_{\phi f \bar{f}} \frac{m_f}{v} \bar{f} f \phi^0 - \sum_{V=W,Z} g_{\phi V V} \frac{2M_V^2}{v} V_\mu V^\mu \phi^0, \quad (1)$$

where ϕ^0 can be h^0 or H^0 . The couplings of ϕ^0 to the fermions and vector bosons are $g_{\phi f \bar{f}}$ and $g_{\phi V V}$, respectively. m_f and M_V are masses of the fermions and vector bosons, respectively. Moreover, $g_{h f \bar{f}} = g_{h V V} = 1$ and $g_{H f \bar{f}} = g_{H V V} = 0$ in the SM and $v = \sqrt{v_1^2 + v_2^2} \sim 246 \text{ GeV}$. The ϕ^0 coupling to gauge bosons is the same for all four models considered here, while the couplings to fermions differentiates between the models. The couplings of h^0 and H^0 to fermions and gauge bosons relative to the SM couplings are given for all four 2HDMs in Table I and Table II, respectively. Many papers [6–36] examined various channels in the four 2HDMs in light of the experimental findings at the LHC and ILC. In this paper, we study constraints on the parameter space in 2HDMs using current Higgs coupling measurements as well as heavy Higgs searches at the LHC, the extension of these limits to 300 fb^{-1} and 3000 fb^{-1} , and projections for the ILC at the center of mass energy (\sqrt{s}) 250, 500 and 1000 GeV.

II. LHC REACH FROM h^0 MEASUREMENTS

We have shown the results with the most recent experimental data and have also studied the bounds that can be obtained at a future LHC with 14 TeV and integrated luminosities of 300 fb^{-1} and 3000 fb^{-1} . To estimate these bounds, we look at the current errors, assume that the SM prediction is correct, and scale the errors as $1/\sqrt{N}$, where N scales like the integrated luminosity. This corresponds to ‘scheme 2’ of the CMS[37] high luminosity projections.

A χ^2 fit to the data shown in Tables III and IV is performed assuming $M_{h^0} = 125 \text{ GeV}$. We follow the standard definition of $\chi^2 = \sum_i \frac{(R_i^{2HDM} - R_i^{\text{meas}})^2}{(\sigma_i^{\text{meas}})^2}$, where R^{2HDM} represents predictions for the signal strength from the 2HDMs

TABLE I: Light Neutral Higgs (h^0) Couplings in the 2HDMs

	I	II	Lepton Specific	Flipped
g_{hVV}	$\sin(\beta - \alpha)$	$\sin(\beta - \alpha)$	$\sin(\beta - \alpha)$	$\sin(\beta - \alpha)$
$g_{ht\bar{t}}$	$\frac{\cos \alpha}{\sin \beta}$	$\frac{\cos \alpha}{\sin \beta}$	$\frac{\cos \alpha}{\sin \beta}$	$\frac{\cos \alpha}{\sin \beta}$
$g_{hb\bar{b}}$	$\frac{\cos \alpha}{\sin \beta}$	$-\frac{\sin \alpha}{\cos \beta}$	$\frac{\cos \alpha}{\sin \beta}$	$-\frac{\sin \alpha}{\cos \beta}$
$g_{h\tau^+\tau^-}$	$\frac{\cos \alpha}{\sin \beta}$	$-\frac{\sin \alpha}{\cos \beta}$	$-\frac{\sin \alpha}{\cos \beta}$	$\frac{\cos \alpha}{\sin \beta}$

TABLE II: Heavy Neutral CP Even Higgs (H^0) Couplings in the 2HDMs

	I	II	Lepton Specific	Flipped
g_{HVV}	$\cos(\beta - \alpha)$	$\cos(\beta - \alpha)$	$\cos(\beta - \alpha)$	$\cos(\beta - \alpha)$
$g_{Ht\bar{t}}$	$\frac{\sin \alpha}{\sin \beta}$	$\frac{\sin \alpha}{\sin \beta}$	$\frac{\sin \alpha}{\sin \beta}$	$\frac{\sin \alpha}{\sin \beta}$
$g_{Hb\bar{b}}$	$\frac{\sin \alpha}{\sin \beta}$	$\frac{\cos \alpha}{\cos \beta}$	$\frac{\sin \alpha}{\sin \beta}$	$\frac{\cos \alpha}{\cos \beta}$
$g_{H\tau^+\tau^-}$	$\frac{\sin \alpha}{\sin \beta}$	$\frac{\cos \alpha}{\cos \beta}$	$\frac{\cos \alpha}{\cos \beta}$	$\frac{\sin \alpha}{\sin \beta}$

and R^{meas} stands for the measured signal strength shown in Tables III and IV.

Our results are given in Fig. 1.

- For each of the four models, we plot the current limits on the parameter space, and the projected limits for integrated luminosities of 300 fb^{-1} and 3000 fb^{-1} . Bounds from flavor physics constrain $\tan \beta \geq 1$ [7, 38] and we take this as a prior when we determine the chi-squared minima.
- In all of the models the minimum of the χ^2 occurs for $\tan \beta \sim 1$ and $\cos(\beta - \alpha) \sim 0$, demonstrating that the couplings of a 2HDM are already constrained to be close to the SM values.
- The parameter space for the type-I model is not very constrained at present. This is because, in the large $\tan \beta$ limit, $g_{hf\bar{f}} = \frac{\cos \alpha}{\sin \beta} \approx \cos \alpha$, which is independent of $\tan \beta$. Increasing the integrated luminosity will gradually narrowed the allowed parameter space in the large $\tan \beta$ limit,
- The lepton specific model is also not severely constrained, because of the enhanced decay to τ leptons, which is poorly measured at present. For large $\tan \beta$, the bottom-quark Yukawa coupling becomes substantial in the type-II and flipped models, and thus the currently allowed parameter space is much more restricted.

III. CONSTRAINTS FROM HEAVY HIGGS SEARCHES

ATLAS [39] and CMS [40] have obtained upper bounds on the ratio of the production cross section to the SM expectation for a SM Higgs boson in various decay channels with a mass between 150 and 600 GeV and assuming a SM width. We use the 95% confidence level band from recent CMS bounds (from Figure 11 in Ref.[40]) and scale predictions as the inverse square root of the integrated luminosity. For example, suppose M_{H^0} is 200 GeV. A SM Higgs boson of 200 GeV will decay almost 100% of the time into vector bosons. This is also true (except for extreme values of the parameters) in a 2HDM. The production rate through gluon fusion in 2HDM will be different than the SM rate because of the different t and b couplings. Thus, the upper bound from ATLAS and CMS on the cross section relative to the SM rate will place a constraint on α and β .

We find that the best constraint comes from $M_{H^0} = 200 \text{ GeV}$, and therefore we will just show the result at this mass point. More detailed analyses can be found in Ref.[25]. For $M_{H^0} = 200 \text{ GeV}$, the results are summarized in Fig. 2. We show results for the type-I and type-II models, with the current limits and projections for 300 fb^{-1} and 3000 fb^{-1} .

- The lepton specific and flipped models give very similar results to the type-I and type-II models, respectively. An increase in luminosity will tightly constrain $\cos(\beta - \alpha)$ for $\tan \beta < 4$ in the type-I model and will give a significant constraint for $\tan \beta < 4$ in the type-II model.
- We see that even with current bounds, a significant fraction of the previously allowed parameter space in the type-I model is excluded by the heavy Higgs search results, and this fraction grows with increasing integrated

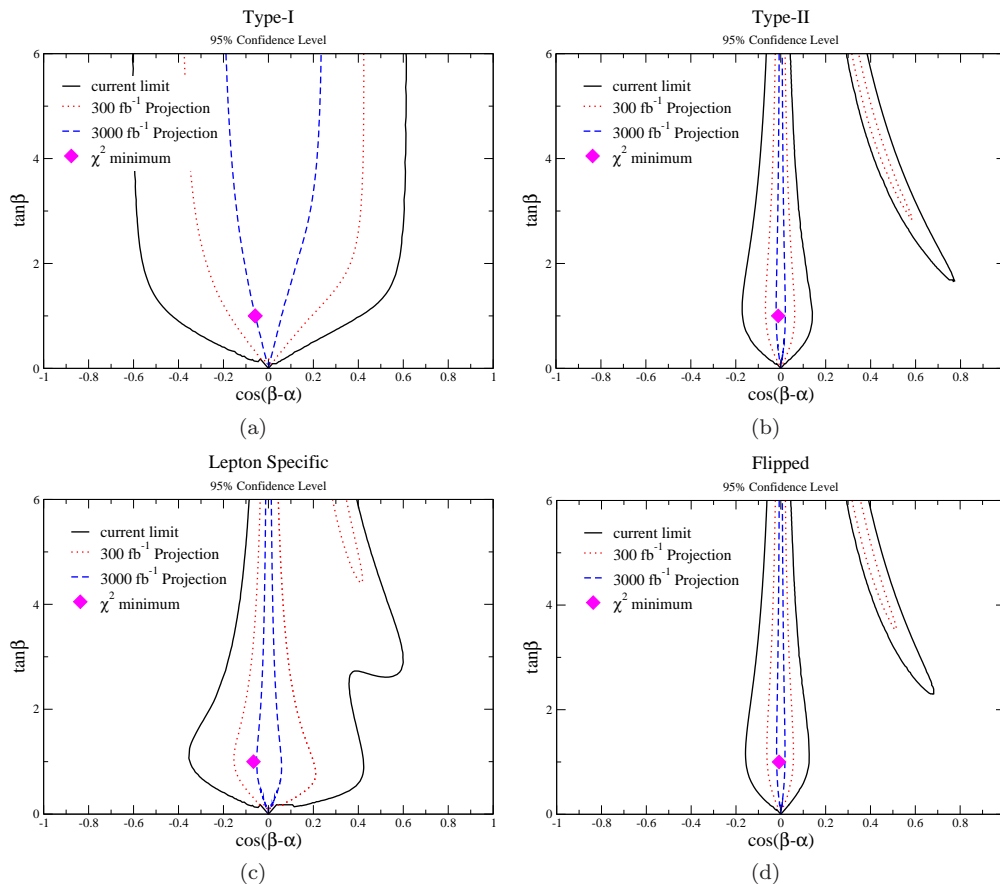


FIG. 1: Allowed regions in the $(\cos(\beta - \alpha), \tan\beta)$ plane in type-I (a), type-II (b), Lepton Specific (c), and Flipped (d) 2HDMs obtained by performing a χ^2 analysis. The region between the black (solid), red (dotted), and blue (dashed) lines is allowed at 95% confidence level corresponding to the current limits and the projected limits for integrated luminosities of 300 fb^{-1} and 3000 fb^{-1} , respectively.

luminosity (unless, of course, the heavy Higgs is discovered). For the type-II model, some of the remaining parameter space is excluded, especially for small $\tan\beta$. This is a significant result, and shows that the allowed parameter space of a 2HDM can be substantially narrowed by considering bounds from heavy Higgs searches.

IV. CONSTRAINTS FROM THE ILC

The ILC has great potential to precisely measure the total width and mass of the discovered Higgs. It is important to study the projected sensitivity at the ILC and its constraints on the parameter space of 2HDMs. The design center of mass energy at the ILC are 250 and 500 GeV with a possibility to upgrade to 1 TeV. The corresponding integrated luminosities are 250, 500 and 1000 fb^{-1} , respectively. In the following, we will use the notations:

- ILC1: data collected from ILC at $\sqrt{s} = 250 \text{ GeV}$ with a luminosity of 250 fb^{-1} .
- ILC2: ILC1 plus data collected from ILC at $\sqrt{s} = 500 \text{ GeV}$ with a luminosity of 500 fb^{-1} .
- ILC3: ILC2 plus data collected from ILC at $\sqrt{s} = 1000 \text{ GeV}$ with a luminosity of 1000 fb^{-1} .

The uncertainties used in our χ^2 analysis are taken from Table 2 of Ref.[41], which can also be found in Ref.[42]. It is very interesting to compare future projections for the LHC and ILC, as shown in Fig. 3.

- In the type-I model, ILC2 already improves the limit a lot compared with that from LHC light higgs measurements. Limits from ILC3 further restrict the parameter space a bit. Furthermore, bounds from the heavy Higgs search are very restrictive at low $\tan\beta$ ($\tan\beta < 4$).

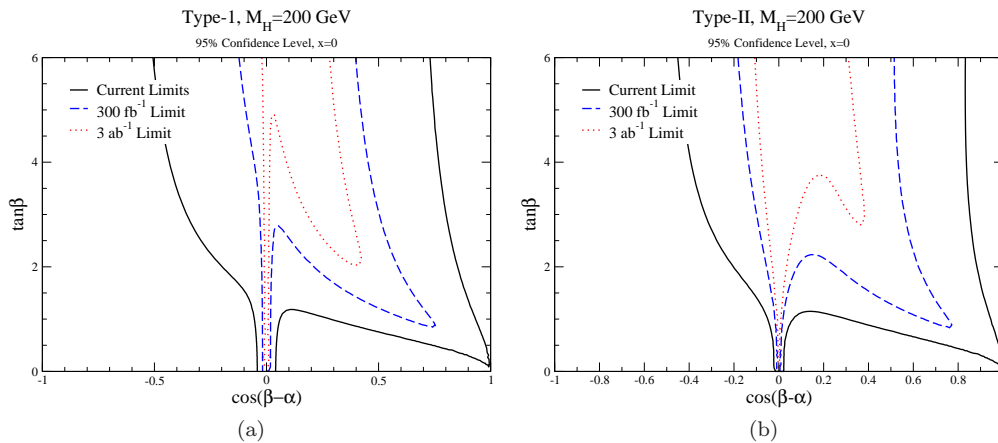


FIG. 2: Allowed regions in type-I (a) and type-II (b) 2HDMs from the LHC limit on a 200 GeV heavy Higgs boson. The region between the black (solid), blue (dashed) and red (dotted) curves is allowed at 95% confidence level corresponding to the current limits and the projected limits for integrated luminosities of 300 fb^{-1} and 3000 fb^{-1} , respectively.

- In the type-II model, only a small region of the parameter space is allowed at 95% CL. For the large $\tan\beta$ region, limits from the heavy Higgs search at the LHC are weaker compared with those from the coupling measurements at the LHC and ILC, which tightly constrain the parameter space. At low $\tan\beta$, however, constraints from the heavy Higgs searches strongly restrict the parameter space.
- For the lepton specific model, all bounds except for those from the LHC heavy Higgs search are similar in the large $\tan\beta$ region, but bounds from the ILC look slightly restrictive. ILC2 and ILC3 are able to give better limits than those from the LHC light Higgs measurements for $\tan\beta < 4$.
- In the type-II model, the allowed region centers around $\cos(\beta - \alpha) = 1$ and becomes narrower as $\tan\beta$ increases. This is because in this model the Higgs coupling to the b quarks, $g_{hb\bar{b}} = \frac{\sin\alpha}{\cos\beta}$, is proportional to $\sqrt{1 + \tan^2\beta}$. The bound gets stronger when $\tan\beta$ becomes larger. This is also true for the flipped model. As a result, bounds on the parameter space of the type-II and the flipped models are very similar.

V. CONCLUSIONS

In this paper, we examined the projected restrictions on 2HDM parameter space from the LHC with 300 and 3000 fb^{-1} of data. In particular, we focused on the sensitivity obtained via measurements of the 125 GeV Higgs boson production and decay rates, and demonstrated that LHC searches for SM Higgs bosons can be recast as searches for other heavy Higgs bosons of 2HDMs. For the type-I model with a heavy Higgs mass of 200 GeV, the parameter space allowed from branching ratios of the 125 GeV Higgs can be shrunk by more than a factor of two by including bounds from the heavy Higgs searches. It is thus important, in the LHC upgrade, to continue these searches. For all models bounds from heavy Higgs searches are very constraining at low $\tan\beta$ ($\tan\beta < 4$), while they are less restrictive at larger $\tan\beta$. However, bounds from the coupling measurements at the LHC and ILC can constrain the large $\tan\beta$ region very well but are less constraining at low $\tan\beta$. In particular, for the type-I model, the ILC can give more restrictive bounds at large $\tan\beta$. As a consequence, we find that searches at the LHC and ILC are complementary to each other.

Acknowledgments

I would like to thank S. Dawson for suggesting this project and thank Nathaniel Craig, Ian Lewis, and Marc Sher for helpful discussions. This work is supported by the United States Department of Energy under Grant DE-AC02-98CH10886.

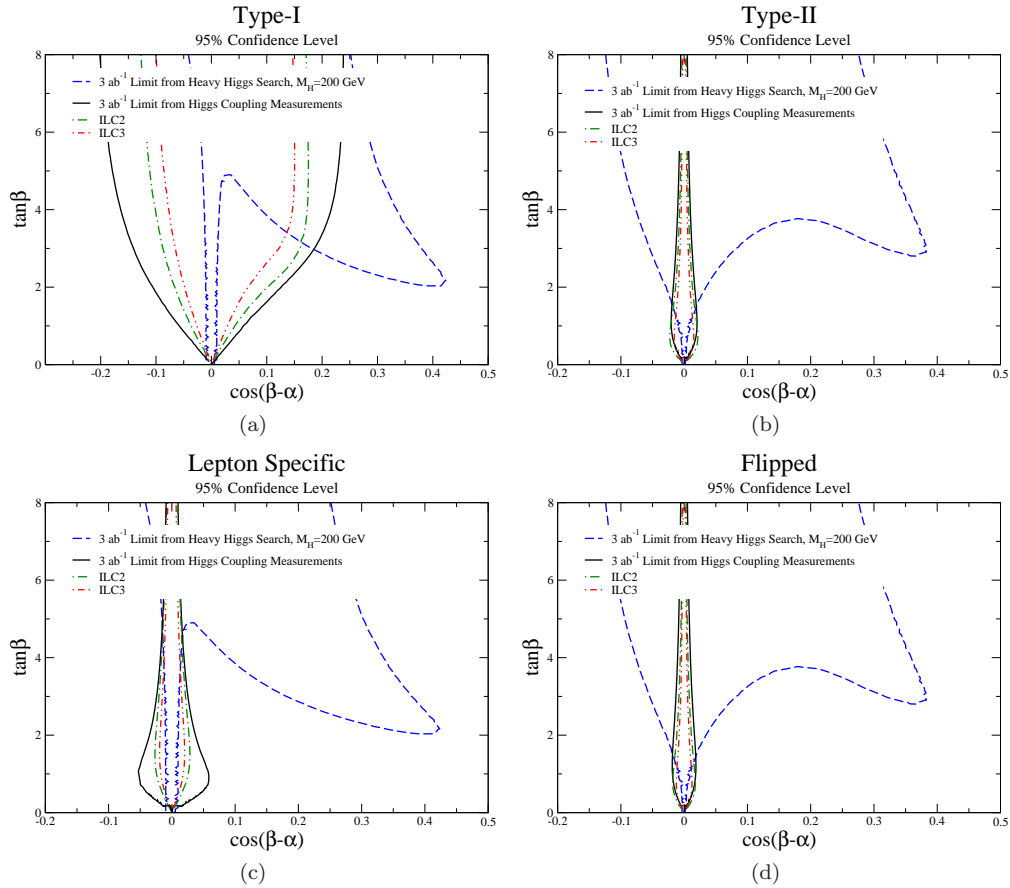


FIG. 3: Allowed regions in the $(\cos(\beta - \alpha), \tan\beta)$ plane in type-I (a), type-II (b), lepton specific (c), and flipped (d) 2HDMs obtained by performing a χ^2 analysis. The region between lines is allowed at 95% confidence level. The black (solid) lines represent the LHC coupling measurements at 3 ab^{-1} . The blue (dashed) lines stand for bounds from heavy Higgs search at 3 ab^{-1} . The green (dot-dashed) and red (double dot-dashed) lines correspond to the projections of ILC2 and ILC3, respectively.

-
- [1] P. M. Ferreira, R. Santos, M. Sher and J. P. Silva, Phys. Rev. D **85**, 035020 (2012) [arXiv:1201.0019 [hep-ph]].
 - [2] A. Drozd, B. Grzadkowski, J. F. Gunion and Y. Jiang, JHEP **1305**, 072 (2013) [arXiv:1211.3580 [hep-ph]].
 - [3] S. Chang, S. K. Kang, J. -P. Lee, K. Y. Lee, S. C. Park and J. Song, JHEP **1305**, 075 (2013) [arXiv:1210.3439 [hep-ph]].
 - [4] G. C. Branco, P. M. Ferreira, L. Lavoura, M. N. Rebelo, M. Sher and J. P. Silva, Phys. Rept. **516**, 1 (2012) [arXiv:1106.0034 [hep-ph]].
 - [5] Y. Grossman, Nucl. Phys. B **426**, 355 (1994) [hep-ph/9401311].
 - [6] P. M. Ferreira, R. Santos, M. Sher and J. P. Silva, Phys. Rev. D **85**, 077703 (2012) [arXiv:1112.3277 [hep-ph]].
 - [7] C. -Y. Chen and S. Dawson, Phys. Rev. D **87**, 055016 (2013) [arXiv:1301.0309 [hep-ph]].
 - [8] D. S. M. Alves, P. J. Fox and N. J. Weiner, arXiv:1207.5499 [hep-ph].
 - [9] N. Craig and S. Thomas, JHEP **1211**, 083 (2012) [arXiv:1207.4835 [hep-ph]].
 - [10] N. Craig, J. A. Evans, R. Gray, C. Kilic, M. Park, S. Somalwar and S. Thomas, JHEP **1302**, 033 (2013) [arXiv:1210.0559 [hep-ph]].
 - [11] Y. Bai, V. Barger, L. L. Everett and G. Shaughnessy, Phys. Rev. D **87**, 115013 (2013) [arXiv:1210.4922 [hep-ph]].
 - [12] A. Freitas and P. Schwaller, Phys. Rev. D **87**, 055014 (2013) [arXiv:1211.1980 [hep-ph]].
 - [13] A. Azatov and J. Galloway, Int. J. Mod. Phys. A **28**, 1330004 (2013) [arXiv:1212.1380 [hep-ph]].
 - [14] B. A. Dobrescu and J. D. Lykken, JHEP **1302**, 073 (2013) [arXiv:1210.3342 [hep-ph]].
 - [15] P. M. Ferreira, H. E. Haber, R. Santos and J. P. Silva, Phys. Rev. D **87**, 055009 (2013) arXiv:1211.3131 [hep-ph].
 - [16] A. Celis, V. Ilisie and A. Pich, JHEP **1307**, 053 (2013) [arXiv:1302.4022 [hep-ph]].
 - [17] B. Grinstein and P. Uttayararat, JHEP **1306**, 094 (2013) arXiv:1304.0028 [hep-ph].
 - [18] J. Shu and Y. Zhang, arXiv:1304.0773 [hep-ph].
 - [19] M. Krawczyk, D. Sokolowska and B. Swiezewska, arXiv:1303.7102 [hep-ph].
 - [20] B. Coleppa, F. Kling and S. Su, arXiv:1305.0002 [hep-ph].

TABLE III: Measured Higgs Signal Strengths

Decay	Production	Measured Signal Strength R^{meas}
$\gamma\gamma$	ggF	$1.6^{+0.3+0.3}_{-0.3-0.2}$, [ATLAS] [43]
	VBF	$1.7^{+0.8+0.5}_{-0.8-0.4}$ [ATLAS][43]
	Vh	$1.8^{+1.5+0.3}_{-1.3-0.3}$ [ATLAS][43]
	inclusive	$1.65^{+0.24+0.25}_{-0.24-0.18}$ [ATLAS][43]
	ggF+ttH	0.52 ± 0.5 [CMS][44]
	VBF+Vh	$1.48^{+1.24}_{-1.07}$ [CMS][44]
	inclusive	$0.78^{+0.28}_{-0.26}$ [CMS][44]
	ggF	$6.1^{+3.3}_{-3.2}$ [Tevatron][45]
WW	ggF	0.82 ± 0.36 [ATLAS] [46]
	VBF+Vh	1.66 ± 0.79 [ATLAS][46]
	inclusive	1.01 ± 0.31 [ATLAS][46]
	ggF	0.76 ± 0.21 [CMS][47]
	ggF	$0.8^{+0.9}_{-0.8}$ [Tevatron][45]
ZZ	ggF	$1.8^{+0.8}_{-0.5}$ [ATLAS] [48]
	VBF+Vh	$1.2^{+3.8}_{-1.4}$ [ATLAS][48]
	inclusive	1.5 ± 0.4 [ATLAS][48]
	ggF	$0.9^{+0.5}_{-0.4}$ [CMS] [49]
	VBF+Vh	$1.0^{+2.4}_{-2.3}$ [CMS][49]
	inclusive	$0.91^{+0.30}_{-0.24}$ [CMS][49]

TABLE IV: Measured Higgs Signal Strengths

Decay	Production	Measured Signal Strength R^{meas}
$b\bar{b}$	Vh	-0.4 ± 1.0 [ATLAS] [50]
	Vh	$1.3^{+0.7}_{-0.6}$ [CMS][51]
	Vh	$1.56^{+0.72}_{-0.73}$ [Tevatron][45]
$\tau^+\tau^-$	ggF	2.4 ± 1.5 [ATLAS][52]
	VBF	-0.4 ± 1.5 [ATLAS][52]
	inclusive	0.8 ± 0.7 [ATLAS][50]
	ggF	0.73 ± 0.50 [CMS][53]
	VBF	$1.37^{+0.56}_{-0.58}$ [CMS][53]
	Vh	$0.75^{+1.44}_{-1.40}$ [CMS][53]
	inclusive	1.1 ± 0.4 [CMS][53]
	ggF	$2.1^{+2.2}_{-1.9}$ [Tevatron][45]

- [21] W. Altmannshofer, S. Gori and G. D. Kribs, Phys. Rev. D **86**, 115009 (2012) [arXiv:1210.2465 [hep-ph]].
- [22] C. -W. Chiang and K. Yagyu, arXiv:1303.0168 [hep-ph].
- [23] L. Basso, A. Lipniacka, F. Mahmoudi, S. Moretti, P. Osland, G. M. Pruna and M. Purmohammadi, JHEP **1211**, 011 (2012) [arXiv:1205.6569 [hep-ph]].
- [24] A. Barroso, P. M. Ferreira, R. Santos, M. Sher and J. Bo P. Silva, arXiv:1304.5225 [hep-ph].
- [25] C. -Y. Chen, S. Dawson and M. Sher, Phys. Rev. D **88**, 015018 (2013) [arXiv:1305.1624 [hep-ph]].
- [26] P. M. Ferreira, R. Santos, M. Sher and J. o P. Silva, arXiv:1305.4587 [hep-ph].
- [27] S. Kanemura, K. Tsumura and H. Yokoya, arXiv:1305.5424 [hep-ph].
- [28] A. Barroso, P. M. Ferreira, I. P. Ivanov and R. Santos, JHEP **1306**, 045 (2013) arXiv:1303.5098 [hep-ph].
- [29] J. Chang, K. Cheung, P. -Y. Tseng and T. -C. Yuan, Phys. Rev. D **87**, 035008 (2013) [arXiv:1211.3849 [hep-ph]].
- [30] N. Craig, J. Galloway and S. Thomas, arXiv:1305.2424 [hep-ph].
- [31] G. Belanger, B. Dumont, U. Ellwanger, J. F. Gunion and S. Kraml, arXiv:1306.2941 [hep-ph].

- [32] V. Barger, L. L. Everett, H. E. Logan and G. Shaughnessy, arXiv:1307.3676 [hep-ph].
- [33] S. D. Rindani, R. Santos and P. Sharma, arXiv:1307.1158 [hep-ph].
- [34] R. V. Harlander, S. Liebler and T. Zirke, arXiv:1307.8122 [hep-ph].
- [35] V. Barger, L. L. Everett, H. E. Logan and G. Shaughnessy, arXiv:1308.0052 [hep-ph].
- [36] D. Lopez-Val, T. Plehn and M. Rauch, arXiv:1308.1979 [hep-ph].
- [37] CMS Collaboration, CMS Note 2012-006.
- [38] F. Mahmoudi and O. Stal, Phys. Rev. D **81**, 035016 (2010) [arXiv:0907.1791 [hep-ph]].
- [39] G. Aad *et al.* [ATLAS Collaboration], Phys. Lett. B **716**, 1 (2012) [arXiv:1207.7214 [hep-ex]].
- [40] S. Chatrchyan *et al.* [CMS Collaboration], arXiv:1304.0213 [hep-ex].
- [41] M. E. Peskin, arXiv:1207.2516 [hep-ph].
- [42] C. Adolphsen, M. Barone, B. Barish, K. Buesser, P. Burrows, J. Carwardine, J. Clark and Hln. M. Durand *et al.*, arXiv:1306.6353 [physics.acc-ph].
- [43] ATLAS Collaboration, ATLAS-CONF-2013-012.
- [44] CMS Collaboration, CMS PAS HIG-13-001.
- [45] See talk slides, ‘H \rightarrow bb from Tevatron’, by Yuji Enari, at HCP2012.
- [46] ATLAS Collaboration, ATLAS-CONF-2013-030.
- [47] CMS Collaboration, CMS PAS HIG-13-003.
- [48] ATLAS Collaboration, ATLAS-CONF-2013-013.
- [49] CMS Collaboration, CMS PAS HIG-13-002.
- [50] ATLAS Collaboration, ATLAS-CONF-2012-170.
- [51] CMS Collaboration, CMS PAS HIG-12-044.
- [52] ATLAS Collaboration, ATLAS-CONF-2012-160.
- [53] CMS Collaboration, CMS PAS HIG-13-004.